Journal of Hazardous Materials 460 (2023) 132516

Contents lists available at ScienceDirect

Journal of Hazardous Materials

journal homepage: www.elsevier.com/locate/jhazmat

Hazardous particles during diesel engine cold-start and warm-up: Characterisation of particulate mass and number under the impact of biofuel and lubricating oil

Ali Zare[a,*], Meisam Babaie[b], Alireza Shirneshan[c,d], Puneet Verma[e], Liping Yang[f], Zoran D. Ristovski[g,h], Richard J. Brown[g], Timothy A. Bodisco[g,i], Svetlana Stevanovic[a]

[a] School of Engineering, Deakin University, VIC 3216, Australia
[b] School of Mechanical Engineering, University of Leeds, Leeds, United Kingdom
[c] Department of Mechanical Engineering, Najafabad Branch, Islamic Azad University, Najafabad, Iran
[d] Aerospace and Energy Conversion Research Center, Najafabad Branch, Islamic Azad University, Najafabad, Iran
[e] School of Populations and Global Health, The University of Western Australia, Perth, WA 6009, Australia
[f] Institute of Power and Energy Engineering, Harbin Engineering University, No. 145-1, Nantong Street, Nangang District, Harbin 150001, China
[g] Biofuel Engine Research Facility, Queensland University of Technology (QUT), QLD 4000 Australia
[h] International Laboratory for Air Quality and Health, Queensland University of Technology (QUT), QLD 4000, Australia
[i] University of Sydney, Sydney, NSW, Australia

HIGHLIGHTS

- This research evaluated particle emission characteristics.
- This study used biofuel and lubricating oil.
- Cold-start, hot-start, and two intermediate warm-up phases were studied.
- Particles in nucleation mode elevated during the engine warmed up.
- Using 5% lubricating oil increased the nucleation mode particles significantly.

GRAPHICAL ABSTRACT

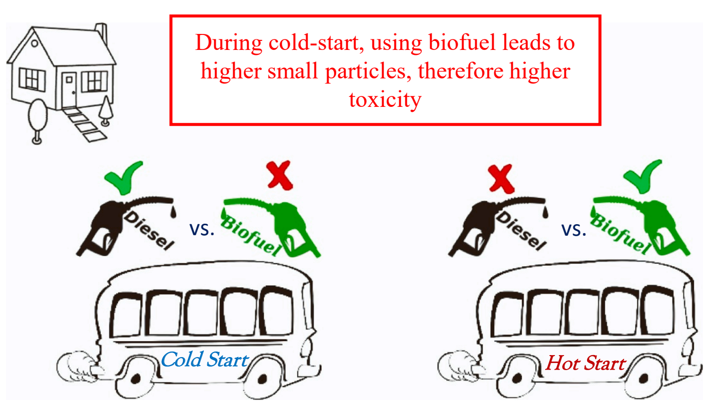

ARTICLE INFO

Editor: Zaher Hashisho

Keywords:
Cold-start
Diesel engine
PN and particle size distribution

ABSTRACT

The increasing share of using biofuels in vehicles (mandated by current regulations) leads to a reduction in particle size, resulting in increased particle toxicity. However, existing regulations disregarded small particles (sub-23 nm) that are more toxic. This impact is more significant during vehicle cold-start operation, which is an inevitable frequent daily driving norm where after-treatment systems prove ineffective. This study investigates the impact of biofuel and lubricating oil (as a source of nanoparticles) on the concentration, size distribution, median diameter of PN and PM, and their proportion at size ranges within accumulation and nucleation modes

* Corresponding author.
E-mail addresses: ali_z4688@yahoo.com, ali.zare@deakin.edu.au (A. Zare).

https://doi.org/10.1016/j.jhazmat.2023.132516
Received 6 July 2023; Received in revised form 25 August 2023; Accepted 7 September 2023
Available online 9 September 2023
0304-3894/© 2023 The Author(s). Published by Elsevier B.V. This is an open access article under the CC BY license (http://creativecommons.org/licenses/by/4.0/).

Lubricating oil
Biofuel

during four phases of cold-start and warm-up engine operation (diesel-trucks/busses application). The fuels used were 10% and 15% biofuel and with the addition of 5% lubricating oil to the fuel. Results show that as the engine warms up, PN for all the fuels increases and the size of particles decreases. PN concentration with a fully warmed-up engine was up to 132% higher than the cold-start. Sub-23 nm particles accounted for a significant proportion of PN (9%) but a smaller proportion of PM (0.1%). The fuel blend with 5% lubricating oil showed a significant increase in PN concentration and a decrease in particle size during cold-start.

1. Introduction

The transportation industry is currently experiencing a substantial move towards low- and zero-emission vehicles; various approaches and technologies are being implemented to reduce harmful emissions from burning fossil fuels in internal combustion engines [1]. Currently, the main approaches are electrification and using hydrogen fuel cells in vehicles; however, these can take years to be fully implemented. During this transition period, there are measures to control and mitigate the adverse impact of emissions from vehicles with internal combustion engines on the environment and human health. One particular strategy is focused on fuel choice.

In the transportation sector, the negative impact of fossil fuels has garnered considerable attention and interest in renewable alternatives, such as biofuels. To promote the use of renewable alternatives, incentives have been introduced. As an example, Directive 2003/30/EC was introduced with the objective of elevating the proportion of biofuels to 5.75% by 2010, whereas Directive 2009/28/EC sought to further amplify the share to 10% by 2020. The current Euro 6.2 (WLTP) regulation uses 10% biodiesel in the market fuel.

Using biofuel in transportation has some advantages in terms of engine performance [2–5] and exhaust emissions [6–8]. For example, the use of biofuels, such as waste cooking biodiesel, holds promise in enhancing the efficiency of diesel engines (thermal efficiency, and some cases, mechanical efficiency) compared to conventional diesel [9]. However, the extent of the improvement depends on the specific biofuel used [10,11]. The lubricity of biofuels, such as waste cooking oil, is superior to that of diesel, resulting in lower friction parameters [12]. However, biofuel blends have been found to have higher fuel consumption and lower power due to their lower calorific value, higher density and higher viscosity [13,14]. Biofuels have been found to produce lower hydrocarbon (HC) and carbon monoxide (CO) emissions but higher nitrogen oxides (NOx) emissions compared to diesel [15,16]; however, the use of after-treatment systems, such as exhaust gas recirculation (EGR), can help to address the NOx issues [13]. One of the most significant advantages of using biofuels (first-generation) is the substantial reduction in PM emissions because of their oxygen content [17,18].

Particulate matter emissions are complex pollutants composed of solid and liquid mixtures in exhaust fumes. Due to their chemical composition and formation, they are recognised as a global risk factor, posing a significant environmental threat. Studies have linked them to human cardiorespiratory issues [19–21]. Furthermore, prolonged exposure to such emissions has been shown to increase free-radical levels, which can negatively impact health [22–26]. The evaluation of particulate matter emissions involves two interrelated perspectives. The first perspective involves the measurement of particulate mass—PM. PM quantifies the mass of particles released from vehicle exhaust tailpipes. However, relying solely on PM measurement is insufficient in assessing the health risks posed by particles since the smaller and more harmful particles have less or no contribution to PM [27].

On the other hand, PN, which stands for the particulate number, the second perspective, provides more informative insights and has garnered significant attention, leading to its inclusion in recent emissions regulations [28]. The reporting of PN emissions for passenger cars became mandatory in Euro 5 regulations, while there were no regulations concerning PN for Euro 1–4 [28]. PN, representing the number of particles, encompasses small-size particles, including those with minimal weight/contribution to PM.

The use of biofuels impacts PN; some research showed an increase in PN emissions when using biofuels instead of diesel [29], while others have reported lower PN emissions [10,30,31]. However, most studies indicated that using biofuels reduces particle size [32–34]. This is significant because of a link between an increase in toxicity and a decrease in particle size [35]. Nevertheless, current regulations, such as Euro 5 and Euro 6, have established a PN measurement guideline and amended their particle measuring method (PMP) to include PN emissions and limit them; however, it still ignores sub-23 nm. It should be noted that the upcoming Euro VII emissions regulation standard, anticipated to become effective in 2025 (although there are discussions about extending this timeline), will encompass more stringent constraints on released particles. Following the approach pioneered by the European Automobile Manufacturers' Association (ACEA), the limitations on emitted particle numbers will encompass particles larger than 10 nm in diameter. These particles must not surpass the previous limit of 6×10^{11} #/kWh [36]. Several research initiatives, like the "DownToTen" project in Europe [37], along with articles [38,39] in relevant literature, have focused on the analysis and measurements of sub-23 nm particles.

PMP considers a count efficiency of 90% (D90) at 41 nm. It also considers 50% (D50) at 23 nm. The literature has reported that changing D50 with smaller sizes (e.g. 10 nm) in PMP for vehicle emissions tests can increase PN significantly. For instance, Leach et al. [40] stated that replacing D90 and D50 with 23 and 10 nm led to a 36% increase in PN. The growing use of biofuels in vehicles, which can increase small PN (e.g. sub-23 nm, which are not included in the regulation), emphasises further investigations on PN emissions and their characteristics and sources in more detail.

Kittelson and colleagues [41] conducted research indicating that the presence of sulphur in lubricating oil led to an increase in nanoparticles. In addition, it is reported that the lubricating oil ash and metal contents are correlated to particle emissions [42,43]. Particles in the nucleation mode, which primarily emerge while exhaust gas is cooling and diluting, consist of organic fractions that are both volatile and soluble. These fractions arise from the lubricating oil and fuel that have not undergone the oxidation process [44]. Our study investigates how lubricating oil presence in the cylinder can impact particulate matter emissions during combustion. The study achieves this by mixing lubricating oil with the biofuel blend and examining its effects on particle matter emissions characteristics.

Excessive emissions can be controlled by after-treatment systems [45], such as diesel particulate filters (DPFs), which are specifically designed to reduce PM emissions [1]. However, the effectiveness of such systems in cold-start operation when the engine is not sufficiently warmed up is still a concern [1]. This is because, for many vehicles, the cold-start operation is a common occurrence, especially during the morning and afternoon commuting to and from work. A considerable number of trips have been reported to start and finish during this period [46]. An instance of this is a research study that analysed over a thousand trips and found that > 30% of them began and ended during cold-start operations [47].

EU Directive 2012/46/EU defines the period of cold-start from the engine start, following 12-hour soaking, for the first 5 min or until the temperature of coolant reaches 70 degC, whichever occurs first. During this period, the combustion process is impacted because of the low/sub-optimal temperature of the engine, which results in different engine emissions and performance compared to hot operation [48,49]. Several research investigations have indicated that cold-start fuel consumption and friction power are higher, as the elevated lubricating oil viscosity at lower temperatures can disadvantage the friction and, consequently, more fuel consumption in order to sustain the engine brake power [46, 50]. Additionally, lower engine/fuel temperatures within cold-start affect fuel evaporation and atomisation, impacting vehicle performance and emissions [51,52].

According to previous works [53,54], emissions are higher within cold-start. For instance, one study showed that PN with biofuels increased significantly during the cold-start section of a custom driving cycle [32]. Another study reported that during cold-start—the first 12% of the LA92 Unified Driving Cycle, the particulate matter emissions were 7.5 times more than Phase 3—hot-start [55]. PN emissions are higher even at low ambient temperatures [56].

While there are some research about NOx, CO_2 and CO emissions [46,57–61], only a limited number of studies have looked in detail at PN and PN size distribution within cold-start [62]. Most of the investigations on cold-start emissions used driving cycles with abrupt load/speed changes, like NEDC or WLTC, and presented average values and not detailed results, which limits the fundamental study. Therefore, it is crucial to limit the number of variables (e.g. engine load/speed) when examining the influence of cold-start and engine temperature on exhaust emissions such as PN. Using constant speed/load, this study will examine the different stages of cold-start and engine warm-up and their respective effects on the particulate number and mass characteristics.

This fundamental research aims to investigate the effects of biofuel, lubricating oil and transient engine temperatures during engine warm-up stages, which includes the cold-start period, on particulate matters. The research will analyse PN, PM and PN median diameter and size distribution, and the particle share at various sizes (e.g. accumulation/nucleation/sub-23) from different perspectives. While previous research has touched on the relationship between lubricating oil and particle emissions [63], this study appears to be the first to specifically investigate the impact of lubricating oil on particle emissions and size distribution of particles within warm-up operations (including cold-start) when biofuel blends are used. This makes the study particularly significant for understanding the potential environmental and health impacts of biofuel and lubricating oil during the combustion process. Not only from the impact of lubrication oil point of view but also the significance of this study stems from the growing usage of biofuel in the market, which is associated with an increase in toxicity as a result of a decrease in particle size when biofuel is used. By comparing the current market blending ratio of 10% and also the next step (15% blending ratio), this study can serve as a reference for car manufacturers and engine researchers to meet upcoming emissions regulations such as Euro 7, where biofuel usage and particle size are of growing importance. In the upcoming regulations, small particles, such as sub-23 nm, are of significant importance, and including such sizes in the vehicle type approval process can lead to certification and homologation test failures; therefore, it is very important to look at the source of such small particles such as biofuels and lubricating oil.

2. Methodology

As can be seen in Table 1, this study used a turbocharged six-cylinder Cummins ISBe220 (common-rail injection) and a hydraulic dynamometer to control the engine load and speed. The engine used in this study did not use any after-treatment system. The reason was to study the pure impact of fuel properties and engine temperature on particulate matter characteristics. Having an after-treatment can limit the study, given that the emissions would depend on the type and performance of such systems [64–66].

Fig. 1 presents the schematic diagram of the test setup. Dynolog software was used to collect the engine and also the dynamometer data.

Table 1
Specifications of the tested diesel engine:.

Cummins ISBe220 31	
Aspiration	Turbocharged
Maximum power	162 @ 2500 (kW @ rpm)
Maximum torque	820 @ 1500 (Nm @ rpm)
Fuel injection	Common rail
Capacity	5.9 L
Cylinders	6 in-line
Compression ratio	17.3:1
Bore × stroke	102 × 120 (mm)

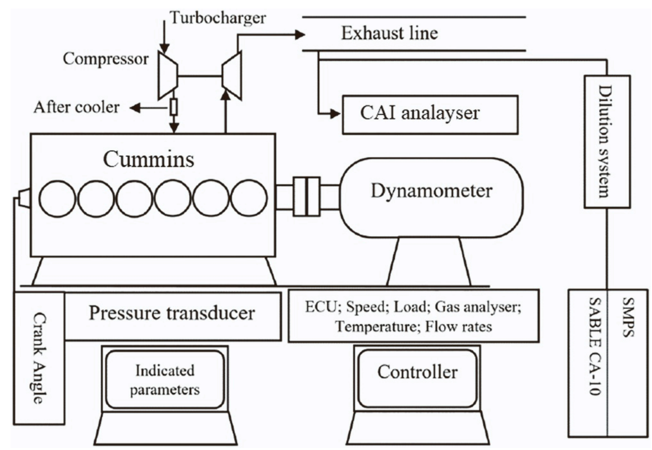

Fig. 1. Schematic diagram of the test setup in this experimental study.

Given that during the engine cold-start and warm-up, the injection strategy changes, the in-cylinder data (e.g. injection signal and crank angle) was measured using a crank angle sensor (Kistler type 2614) and pressure transducer (Kistler 6053CC60) both connected to an A-to-D convertor (DT9832). A National Instruments LabView program was used to record the data [67,68]. The accuracy of the mentioned equipment is shown in Table 2.

This study utilised a scanning mobility particle sizer (SMPS) to measure the particulate matter emissions. The system included a TSI 3071 classifier and TSI 3782 CPC to preselect the particles in various sizes and to grow particles to detectable sizes for the optic, respectively. To measure the emissions during the experiment, the hot exhaust gas (~350 °C) was diluted about 20 times with the HEPA-filtered ambient air at the temperature of ~23 °C within a CVS—constant volume dilution system. A CAI and SABLE CO_2 analysers (Table 2) were used before and after the dilution system to measure the CO_2 and calculate the dilution ratio.

This research investigates particulate matter number and mass, and their size distributions using SMPS which counts particle number in each channel, dividing it by the geometric width of the size of the channel and reporting the normalised concentration. The SMPS Spectrometer

Table 2
The accuracy of instruments used in this experimental study.

Instrument	Unit	Accuracy
Dynamometer	kW	± 0.5%
CAI-600 NDIR CO_2 analyser	ppm	> 0.5%: Linearity > 1% of full scale: Repeatability
Kistler 6053CC60 piezoelectric transducer	pC/bar	≈ ± 20
Kistler type 2614	crank angle degrees	± 0.5
SABLE CA-10 Carbon CO_2 gas analyser	%	1% of reading within the range of 0–10%

Aerosol Instrument Manager Software was used to convert PN to PM and report the normalised particulate mass concentration [69].

As per the literature, ultrafine particles can be categorised by nucleation and accumulation modes based on their size. Particles with a diameter size smaller than 50 nm are typically called nucleation mode particles, and those with a diameter size above 50 nm are categorised in accumulation mode [70]. This study used these two definitions to interpret the data, given that the SMPS measured particles from 10 to 500 nm.

The particles in the exhaust gas include solid particles, and also liquid droplets and volatiles. In PMP, there is a guideline for using a system to remove volatile particles. Such systems use different consecutive stages of hot dilution, heated evaporation tube, and cold dilution, named PND_1, ET and PND_2, respectively (ECE/TRANS/WP.29/GRPE/2016/3 amended by GRPE-72–09-Rev.2). This method is to remove the liquid particles and volatiles ensuring that the particle measurement system only counts solid particles. However, in this study, the measurement is not only limited to solid particles. The size resolution capability of the SMPS can be up to 128 channels per decade—192 channels in total. In terms of measuring sub-23 nm particles and the difficulties related to such measurements [71], it should be mentioned that while the SMPS is capable of measuring such particles and characterising them into different sizes, this instrument is not designed for emissions certification tests (e.g. Euro 6.2) and complying with PMP, due to its time response (Commission Regulation (EU) 2017/2400). Such homologation tests need a particle counter with a high sampling rate (e.g. 10 Hz).

2.1. Fuel selection

This study used neat diesel (D100), D90B10 and D85B15, blends of 0, 10% and 15% biofuel with diesel, respectively. These are the fuels used in the market for different emissions regulations. D100 can represent the past fuels (before Euro 5), and 10 (Euro 6.2) and 15% biofuel blends can be considered as a future blending ratio in the fuel market. This study aimed to investigate the particulate matter emissions within cold-start and warm-up and focused on particles in nucleation mode. The literature has reported that the existence of lubricating oil in the engine during combustion is a significant contributor to nucleation mode particles [63,72–74]. It is reported that the sulphur and phosphorus contents of the lubricating oil [75], as well as the metallic additives originating from lubricating oil [76], were the reason for increased nucleation mode particles. This study artificially added 5% commercial engine lubricating oil into the combustion chamber by mixing it with the fuel blend of diesel and biofuel (D85B10L5), facilitating the evaluation of changes in PN. Given that lubricating oil has a high viscosity, it was decided not to add more than 5% to the fuel blends. In terms of fuel-lubricating oil mixture realism, it is acknowledged and understood that the 5% mixture used may not reflect real-world conditions, and it could be a lower portion depending on the age of the engine; however, this choice allows the analysis of the impact of lubricating oil on emissions, contributing to the broader understanding of emission characteristics. In this study, D, B and L stand for diesel, biofuel and lubricating oil, and the two digits after D, B and L show their volume portion in the blend. For example, D85B10L5 means this fuel blend includes 85% diesel, 10% biofuel and 5% lubricating oil.

Table 3 presents the fuel properties. Trace 1310 Gas chromatograph, a single quadrupole GC-MS System) was utilised to analyse the chemical composition of the fuels. As shown, between the tested fuels, D100 has no cyclic hydrocarbons but the highest aliphatic compounds (low concentration of limonene and alkanes with 7–13 carbons mainly) and aromatic compounds (including mesitylene, xylene, naphthalene, phthalan, and benzene and its derivates). Other fuel blends contained cyclooctane, cyclohexane and cycloalkanes.

It can be seen in Table 3 that the densities of D100, D90B10, D85B15 and D85B10L5 are 0.84, 0.843, 0.845, 0.845 and 0.846, g/cc, respectively. The density of lubricating oil is higher than the other two fuels, and diesel (D100) had the lowest density. For all the fuels in Table 3, the heating value decreases slightly as more biofuel and lubricating oil are added to the blends. The changes are not significant, but it has been reported in the literature that even a small change in fuel properties may have an impact [74]. For example, higher density and lower calorific value of biofuel can adversely impact engine power and fuel economy [12]. Another important parameter that distinguishes biofuels from diesel is the fuel oxygen content, which has been frequently reported as a factor in decreasing PM emissions when biofuel is used as diesel has no oxygen content [24,77]. This could be one of the decision factors for increasing the share of biofuel in the market. When it comes to particulate matter emission, especially small particles, the sulphur content of fuel will be of significant importance as it can be a reason for higher particulate matter emissions [41]. Diesel had 5.9 ppm sulphur content, while the lubricating oil had 7500 ppm, which can lead to higher nucleation mode particles (examined in the Result section). Another fuel property that can make a difference is the higher viscosity of lubricating oil when compared to diesel. This can have an adverse impact on fuel atomisation and evaporation, therefore emissions and performance, especially within cold-start and warm-up, as low temperature leads to higher viscosity [73].

2.2. Design of experiment

This research utilised a constant engine speed (1500 rpm) & 25% engine load to run the cold-start tests. The rationale for selecting a fixed speed/load was to facilitate a study on the pure influence of fuel properties and engine temperature during engine warm-up and cold-start. It is appreciated that there are different ways of conducting cold-start tests, such as using driving cycles (e.g. NEDC, WLTC, etc.); however, such cycles include abrupt speed/load variations that can add additional variables when it comes to data analysis [78–80], and it complicates and limits the fundamental investigations into the pure impacts of engine temperature and fuel properties within the cold-start and warm-up period. Therefore, this study tried to eliminate the effect of speed/load changes by limiting the number of variables via selecting constant engine operation parameters so that it potentially aids a better conclusion. The tested engine had its maximum torque at 1500 rpm, and the reason behind choosing a 25% engine load instead of other typical ones (50%, 75% and 100%) was that when compared to warmed-up operation, within the cold-start and warm-up phases, the engine load is usually lower [81]. An example of this can be WLTC, which is the Euro 6.2 driving cycle designed based on real driving data. In this driving cycle,

Table 3
The properties of fuels used in this experimental study.

	Density at 15 °C (g/cc)	Kinematic viscosity at 40 °C (mm^2/s)	Lower heating value (MJ/kg)	Area%			
				aromatic	oxygenated hydrocarbons	cyclic hydrocarbons	aliphatic
D100	0.84	2.64	41.77	1.43–5.66			1–12.24
D90B10	0.843	2.86	41.31	0.09–0.17	0.19–0.31	0.119–1.12	0.09–0.37
D85B15	0.845	2.97	41.08	0.04–0.10	0.04–0.08	0.04–0.22	0.04–0.74
D85B10L5	0.846	4.24	41.38	0.05–0.08	0.07–0.19		0.05–0.43

the average vehicle speed (combination of engine load and rpm) during the cold-start phase (low phase) is lower than the other parts [81]. For instance, the WLTP Class 3 cycle has four consecutive phases (low--medium-high-extra high, within which the first one can be considered as the cold-start phase) with average speeds of 25.7, 44.5, 60.8 and 94 kph. Comparing these average speed values, it was decided to use a quarter load for cold-start experiments in this study to replicate the real-world condition while keeping the tests simple enough so that it facilitates a fundamental study.

At ambient temperature, the cold-start experiments were conducted daily (consecutive mornings) in an engine laboratory. According to EU Directive 2012/46/EU regulation, the temperatures of engine coolant/oil were checked at the beginning of each test to ensure they were the same as the ambient temperature (23 ± 3 °C). The ambient temperature in the air-conditioned laboratory stayed within the defined boundary (23 ± 5 °C), based on EU Directive 2012/46/EU. For each experiment, the engine was turned on and ran at 1500 rpm under quarter load for at least 60 min till it fully warms up, and meanwhile, the data was recorded. After each test and repeat, in order to use new fuel for the next day, the fuel tank was disconnected, and the engine ran for a while at a high load to flush the fuel pump/lines from the previous fuel. Then, with a new tank of fuel, the engine was run for about an hour to ensure the new fuel was the only fuel that remained in the lines. Then, the engine was soaked for at least 12 h before the new experiment.

The equipment accuracy in this study is shown in Table 2. Error bars are added to the figures in the Result Section, and the experiment repeatability analysis is shown in Table 4. Tests were done twice. As can be seen, the table shows the statistical analysis of test repeatability using a coefficient of variation (CV) between repeated tests during engine cold-start and warm-up. As mentioned, during the experiment, the engine load&speed were constant. The table shows the variation of measured engine speed and load within each test, shown in Test 1 and Test 2 rows. The difference between the tests is low, proving that the tests were repeatable. Also, this study used a high-tech quality CO_2 gas analyser (non-dispersive infrared CAI-600) to measure CO_2 between the tests, evaluating the test repeatability and lab uncertainty, which is a common and trustworthy method in the automotive industry when it comes to emissions laboratory uncertainty measurements.

This study divides the engine warm-up process into four stages based on how the engine coolant and oil warmed up (Appendix, Fig. A1). In brief, Phase 1 represents cold-start, Phases 2 and 3 are intermediate periods between cold-start and hot-start, and Phase 4 represents the engine warmed-up condition. Please refer to the Appendix for details and analysis.

3. Results and discussion

This section analyses the particulate matter emissions by evaluating the total PN, PM and PN median diameter and size distribution, and the variations as the effects of fuel and engine temperature. It also evaluates how the share of sub-23 nm and nucleation mode particles changes under the effects of biofuel and lubricating oil as the engine temperature increases.

Fig. 2 demonstrates the total PN concentration within the engine warm-up phases. As shown, for all the tested fuels, PN during cold-start (Phase 1) has the lowest value and as the engine warms up, PN increases. For example, PN with D100 increased by 52%. One of the main reasons for this increase could be the engine temperature rise, as between the engine operating parameters, the engine speed and load stayed constant, and the engine temperature was increasing. This is similar to another study in the literature [82]. From a fuel properties point of view, the figure illustrates that using 10% and 15% biofuel (D90B10 and D85B15) increases PN emissions in all the phases (this is reported in the literature as well [33,83]. However, adding 5% lubricating oil (D85B10L5) decreases the PN emissions in the first two phases while it increases PN in the last two phases. This shows that the impact of adding lubricating oil to the fuel depends on the engine temperature. This is contradictory to adding biofuel as well, given that the percentage of increase drops as the engine warms up. This will be discussed further by evaluating different particle sizes.

Fig. 3 illustrates the particles' median diameter of particles changes through the four phases of engine warm-up; the size of particles has a slight decrease with biofuel and diesel blends but a significant decrease when using the blend with 5% lubricating oil [84], except in Phase 1. It should be mentioned that similar to PN (Fig. 2), higher variability can be observed in Phase 1.

The literature shows that fuel properties and cold-start have a significant impact on the concentration and size of particulate matter (PN) [85,86]. Hence, the analysis presented here is divided into two sections: the first one will examine the data from the perspective of engine temperature, and the second one will discuss the effects of fuel properties.

3.1. Engine temperature impact

The comparison of PN in Phases 2–4 with cold-start (Phase 1) is presented in Fig. 4(a). The results indicate that the concentration of PN increased in other phases in comparison with Phase 1. As the engine load&speed were maintained constant during Phases 1–4, it can be inferred that the engine temperature played a key role in causing these changes [62,87]. However, it should be noted that while the engine operating parameters (speed and load) remain constant, there are other parameters that can change, such as the start of injection, start of combustion, injection delay, and ignition delay. Fig. 4(a) depicts the temperature of exhaust gas as an engine temperature indicator during all phases. The results show that the exhaust temperature increased through Phases 1–4, but the Phase 3 to Phase 4 change was not as significant as the Phase 1 to Phase 2 change.

Phase 1, with the lowest PN concentration, falls under the cold-start period. In Phase 2, PN increased significantly compared to the first phase, with an increase between 27% and 65%, which was attributed to the changes in injection strategy and engine temperature. In Phase 3, PN was higher than in Phase 1, with an increase of 16–112% for different fuels. Within this Phase 4, PN was higher than in Phase 1, with up to a 132% increase. PN in Phase 3 was slightly different from Phase 4, indicating the impact of the sub-optimal temperature of the lubricating oil despite the optimal coolant temperature. This was more significant (20%) for the fuel with 5% lubricating oil, which means that the engine temperature change had a higher impact when using this fuel. More discussions will be presented in Section 3.2, where the impact of fuel properties is investigated.

Fig. 4(b) illustrates that in comparison to Phase 1, the particles' median diameters rose during the second phase significantly. This is due to the change in the start of injection at this phase, which leads toward incomplete combustion and bigger particles. This trend is followed by a decline in Phases 3 and 4 for each type of fuel. According to existing literature, an increase in nanoparticle concentration is linked to higher exhaust gas temperatures [72]. Therefore, an increase in exhaust

Table 4
Test repeatability analysis: cold-start and warmed-up engine.

			Engine load	Engine speed	CO_2
Cold-start	Coefficient of variation within each test (%)	Test I	3.74	0.15	0.97
		Test II	5.42	0.13	2.27
	Difference between Test 1 and Test II		0.82	0.02	0.12
Warmed-up	Coefficient of variation within each test (%)	Test I	1.34	0.15	0.51
		Test II	1.00	0.14	0.36
	Difference between Test 1 and Test II		1.5	0.04	0.17

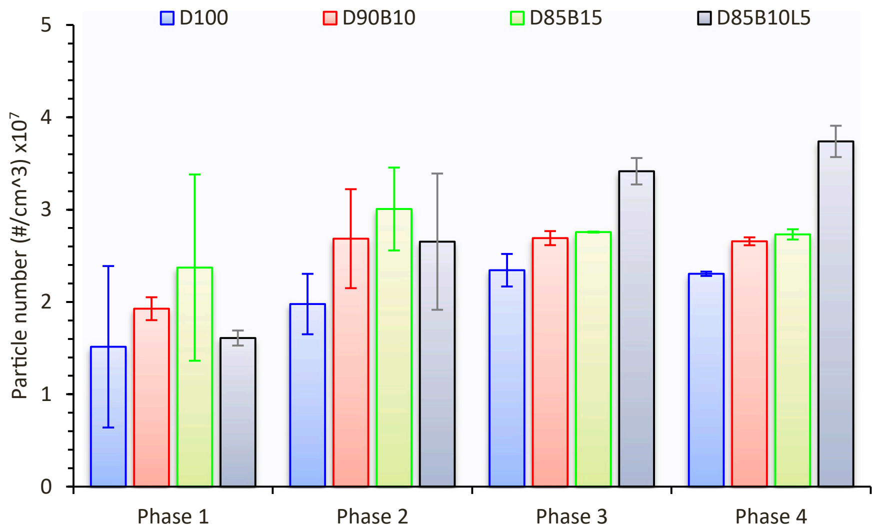

Fig. 2. Total PN within 4 phases of engine warm-up with D100, D90B10, D85B15 and D85B10L5.

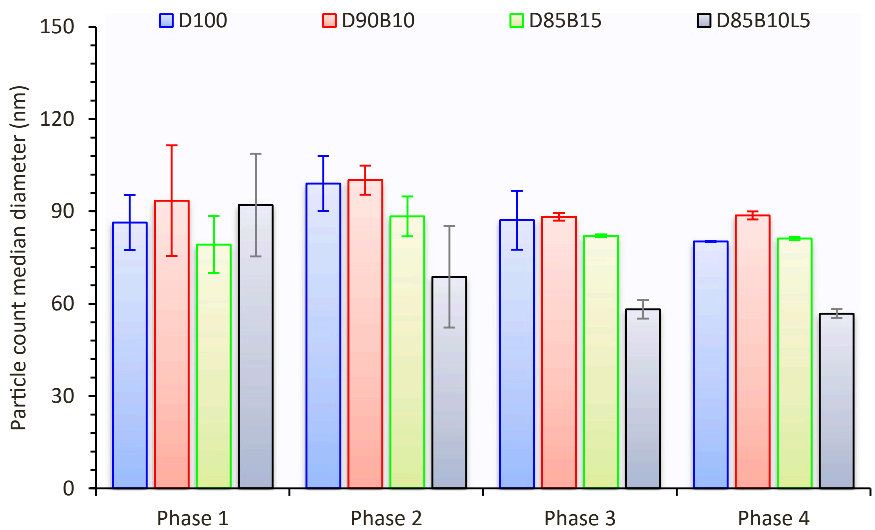

Fig. 3. Particulate number count median diameter within 4 phases of engine warm-up with D100, D90B10, D85B15 and D85B10L5.

temperature from Phase 2 to Phase 4 is linked to a decrease in median diameter. Hence, the characterisation of particle sizes should be further investigated by evaluating the particle size distributions at each phase and for each fuel.

The SMPS used in this study measured particles from 10 to 500 nm; therefore, it cannot consider the large particle sizes. The data presented in Fig. 5(a) and (b) show the size distribution of PN and PM during the engine warm-up. The nucleation mode particles have a negligible contribution to PM but notably to PN. These nanoparticles commonly consist of hydrocarbon or sulphate materials and arise through nucleation as exhaust gases are diluted and cooled. Conversely, accumulation mode particles primarily comprise agglomerates of carbonaceous soot that are directly generated through combustion processes. During the process of exhaust dilution and cooling, volatile substances undergo nucleation, condensation, and adsorption, leading them to transition into solid and liquid particulates. In the hotter confines of the tailpipe, where temperatures are elevated, the majority of volatile components exist in gaseous form. The specific intricacies of the dilution and cooling mechanisms govern the proportions of substances that adhere or condense onto pre-existing particles and initiate nucleation for the creation of fresh particles [70].

Fig. 6(a) and (b) display the PM and PN cumulative share at various size ranges (the SMPS used in this study measured particles from 10 to 500 nm). It shows that, for all fuels and phases, sub-50 nm particles accounted for less than 1% of the total mass, while up to 45% of PN was attributed to sub-50 nm particles. Additionally, sub-30 and sub-23 nm particles accounted for up to 0.1% of the PM cumulative share, while their cumulative PN share was 13% and 9%, respectively, depending on the phase/fuel. Hence, neglecting sub-23 nm particles in current regulations would disregard a considerable number of small and hazardous particles, which is concerning given the volume of automobiles within towns and the PN limitation in regulations. As an example, the threshold of PN from the vehicle homologation test is 6 × 10ˆ11 #/km in Euro 6.2.

Carbonaceous agglomerates and adsorbed materials are the primary contributors to accumulation mode particles, while through the condensation of volatile materials, particles in the nucleation mode can also form particles in the accumulation mode [70]. As shown in Fig. 6(a) and (b), sub-100 nm particles accounted for 50–75% of PN, but only up to 13% of PM. The comparison of Fig. 5(a) and (b) clearly indicates the significant impact of particles larger than 50 nm on the concentration of PM, as evidenced by the size distribution graphs for PN and PM. The influence of particles larger than 100 nm on total PM concentration was

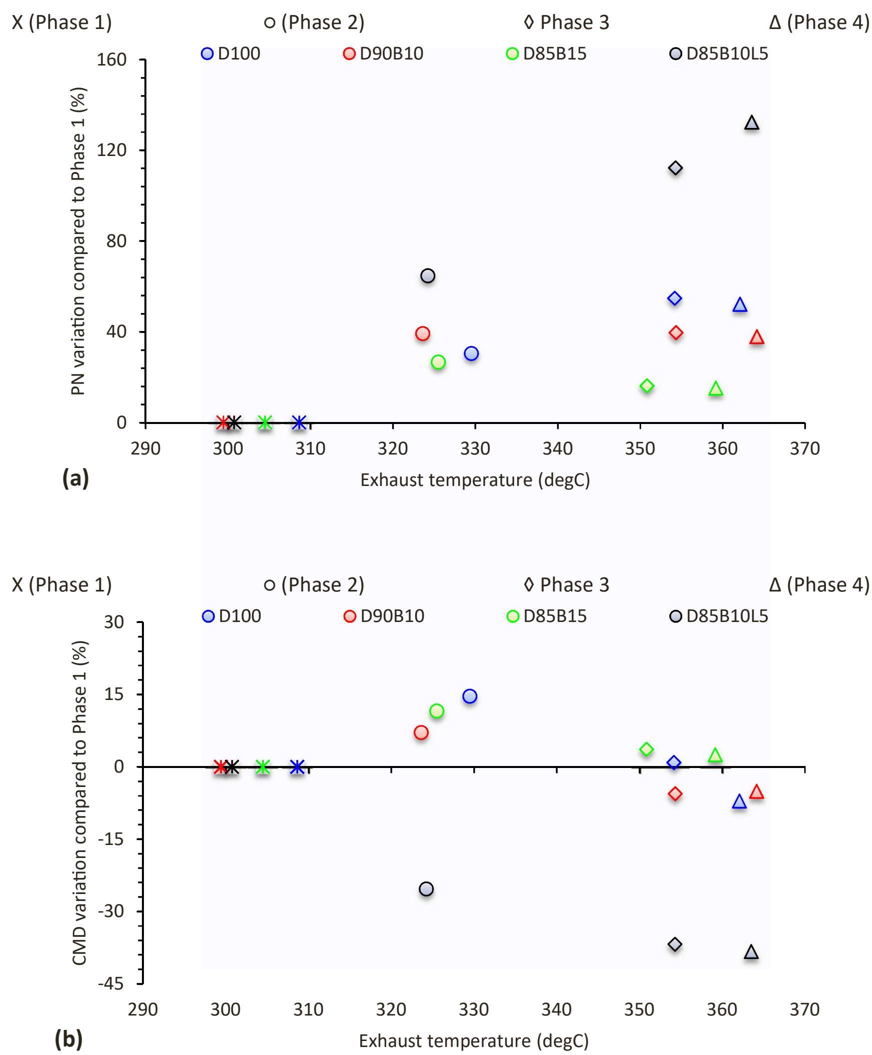

Fig. 4. (a) Particulate number concentration and count median diameter (b) changes compared to Phase 1 at different exhaust temperatures within 4 phases of engine warm-up with D100, D90B10, D85B15 and D85B10L5.

particularly noteworthy, elucidated further by examining Fig. 7, which presents the median diameter of PM in conjunction with Fig. 3, which illustrates the median diameter of PN. The data reveals that the median diameter of particulate mass emissions ranged from 178 up to 213 nm; however, the PN median diameter was from 57 up to 100 nm. These prove that accumulation mode particles have a significant role in particulate mass concentration. Given that the size distribution of particle number and mass from Phase 1 to Phase 4 differs, further investigation is necessary. It should be mentioned that similar to PN count median diameter data (Fig. 3), higher variability can be observed in Phase 1.

Generally, a decrease in particle size indicates a greater proportion of nucleation mode particles. Fig. 3 illustrates the trend of the median diameter, which corresponds to the trend of the nucleation mode particle share in Fig. 6(a) and (b). There is a noticeable increase in the particles' median diameter as they progress through Phase 1 to Phase 2; this can be attributed to the injection strategy shift. However, after that, as the engine warms up, the median diameter gradually decreases. Therefore, an inverse pattern emerges in the distribution of nucleation mode particles; the proportion of particles below 50 nm (and also 23 nm) declines through Phase 1 to Phase 2, before the gradual increase afterwards.

Here is the summary of the observed results during engine warm-up phases (Phases 1–4) in this study. According to Fig. 3, during Phase 1 (formal cold-start), the median diameter of PN was 79–94 nm, depending on the fuel. Fig. 4(b) shows median diameter changes within 4 phases. Fig. 6(a) and (b) show that during Phase 1, a significant portion of PN and a negligible portion of particulate mass are in the nucleation mode. Among them, the proportion of particles with sizes less than 23 nm is up to 13% for PN and 0.1% for PM. Within Phase 1, the exhaust pipe's low temperature decreased the temperature of exhaust gas, and volatile materials homogeneously nucleated into particles during the cooling process. This occurs because a drop in the temperature of exhaust gas can increase the saturation ratio and saturation vapour pressure of volatile materials, leading to condensation and nucleation of volatile materials [88]. VOCs during cold-start are higher than hot-start, as reported in [89], which increases the likelihood of nucleation of particles from the exhaust gas before sampling. This effect is more considerable with biofuels due to their higher VOC content than D100 [90].

Fig. 5(a) and (b) indicate that in Phase 2, as compared to Phase 1, PN is higher and there are bigger particles. This trend is better illustrated in Fig. 4(b), which shows that the median diameter increases from Phase 1 to Phase 2. For instance, with D100, the median diameter of PN increases by 15%. In Phase 2, the shift toward larger particles is also evident by comparing the blue and red colours in Fig. 5(a)—PN cumulative share in the nucleation mode significantly decreased in comparison with Phase 1. For instance, with diesel, the proportion of particles in nucleation mode dropped to 12% from 20%. The proportion of particles

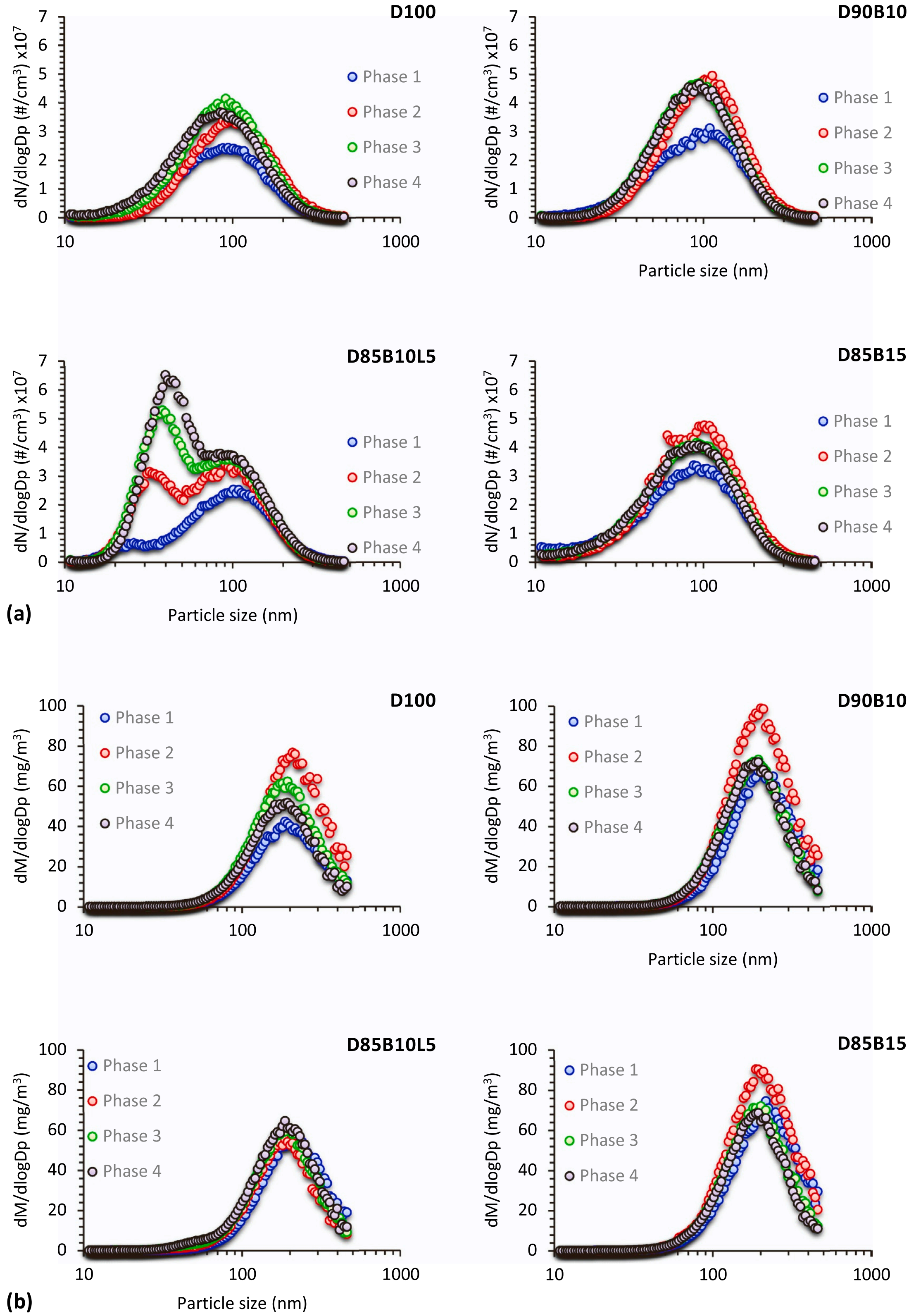

Fig. 5. (a) Particulate number and (b) particulate mass size distributions within 4 phases of engine warm-up with D100, D90B10, D85B15 and D85B10L5.

with sizes less than 23 nm also dropped in Phase 2. During this unsteady warm-up phase, the shift towards larger particles can be attributed to injection strategy variation—the increased start of injection and decreased ignition delay, which negatively influence the atomisation of fuel&premixed combustion. Although the engine temperature was also variable between Phases 1 and 2, it may not be the cause of the increase in particle diameter size. Fig. 4(b) shows that the increasing temperature of the engine may decrease the particle size, as indicated by the declining trend of the median diameter via Phases 2–4. This is relevant to fuel properties, which will be discussed in Section 3.2.

During Phase 3, the particle size distribution graph indicates that the particles were smaller than in Phase 2 but still larger than in Phase 1. In

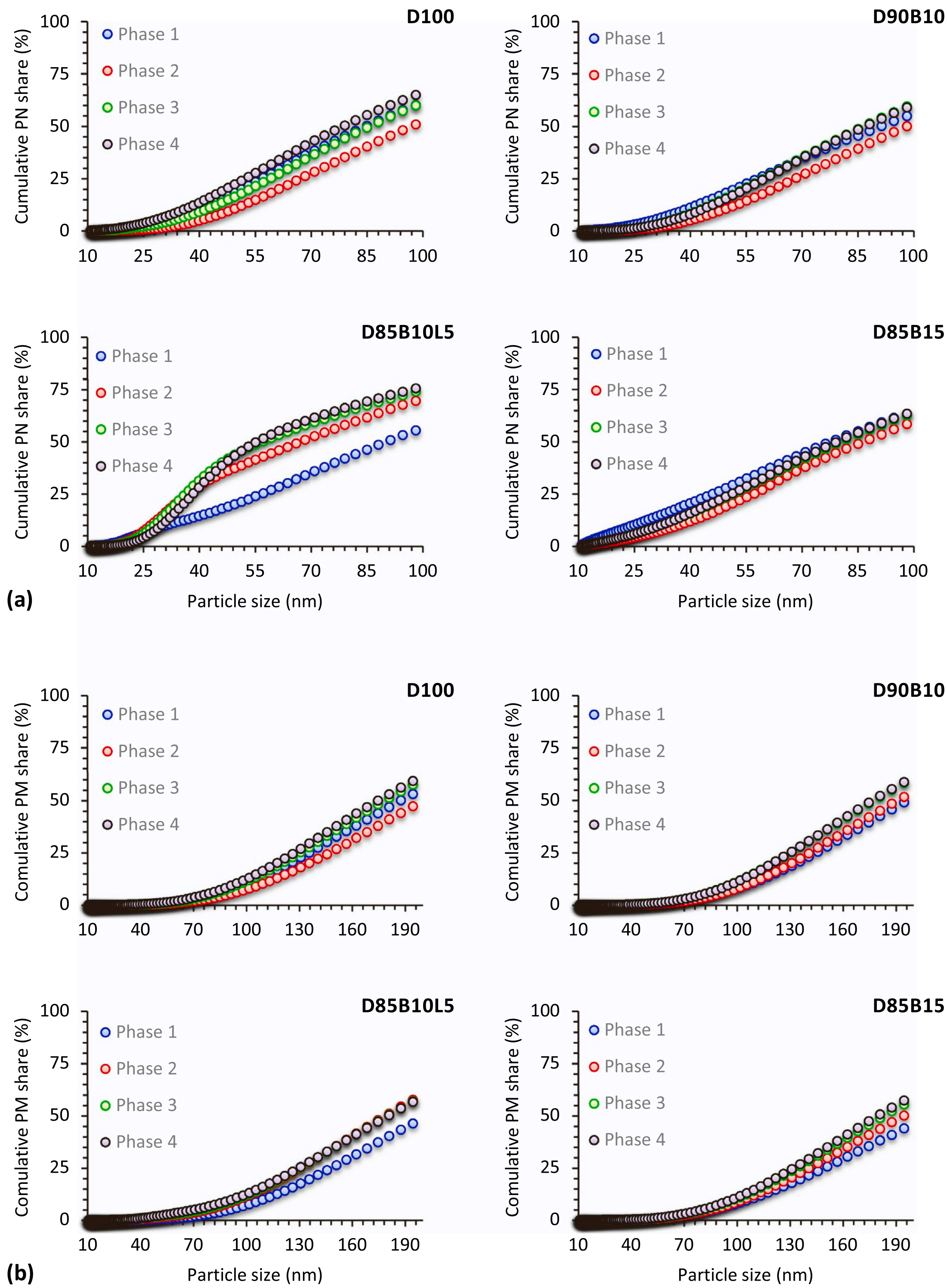

Fig. 6. Cumulative share of (a) particulate number and (b) particulate mass within 4 phases of engine warm-up with D100, D90B10, D85B15 and D85B10L5.

Phase 3, the start of injection remained constant while the engine temperature continued to increase.

When comparing Phase 3 with Phase 2, a correlation becomes evident between the rising exhaust temperature and a decrease in the median diameter of particles. Additionally, there is an observed increase in the proportion of nucleation mode particles in Phase 3 in comparison with Phase 2. It is worth noting, however, that this change was relatively minor for the majority of fuels.

When comparing Phase 4 to both Phase 2 and Phase 3, a notable trend emerges, indicating that the elevated exhaust gas temperature correlates with a reduction in the size of particles, as demonstrated in Fig. 4(b). Moreover, the proportion of particles in the nucleation mode in Phase 4 surpasses that of Phase 3, suggesting that the sub-optimal engine oil temperature in Phase 3 may have contributed to this disparity; however, the change was minor with most fuels, except the one with 5% lubricating oil, which will be discussed in Section 3.2. When comparing Phase 1 to Phase 4, the trend varied with fuels, indicating that the driving factor is likely the properties of fuels.

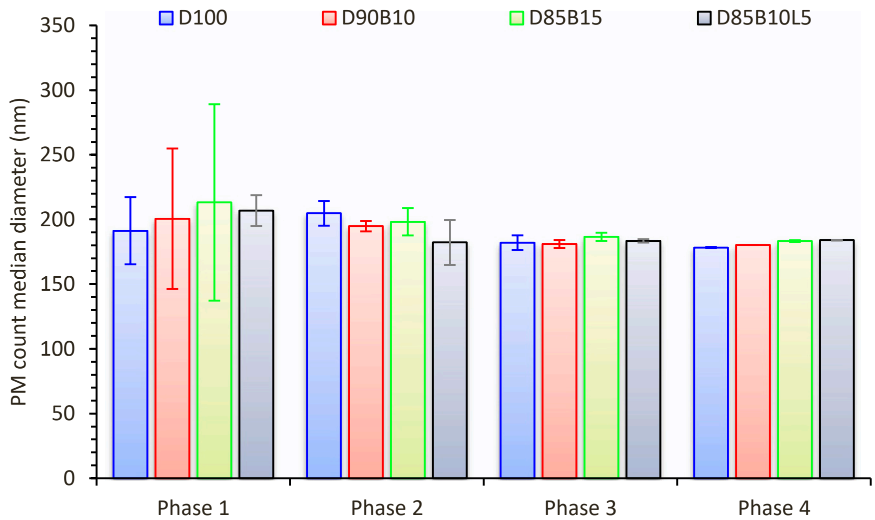

Fig. 7. Particulate mass count median diameter within 4 phases of engine warm-up with D100, D90B10, D85B15 and D85B10L5.

3.2. Fuel impact

It has been frequently reported in the literature that utilising biofuel blends instead of pure diesel impacts the emissions [91–97]; however, this impact can be different under cold-start when compared to hot-operation [53]. In Fig. 2, it was observed that the PN had an increasing trend in all phases when biofuel blends were used compared to diesel. For instance, D85B15 led to a 27%, 16% and 15% increase in PN at Phase 2, Phase 3 and Phase 4 when compared to Phase 1. The reason behind this could be the higher concentration of biofuel VOCs as

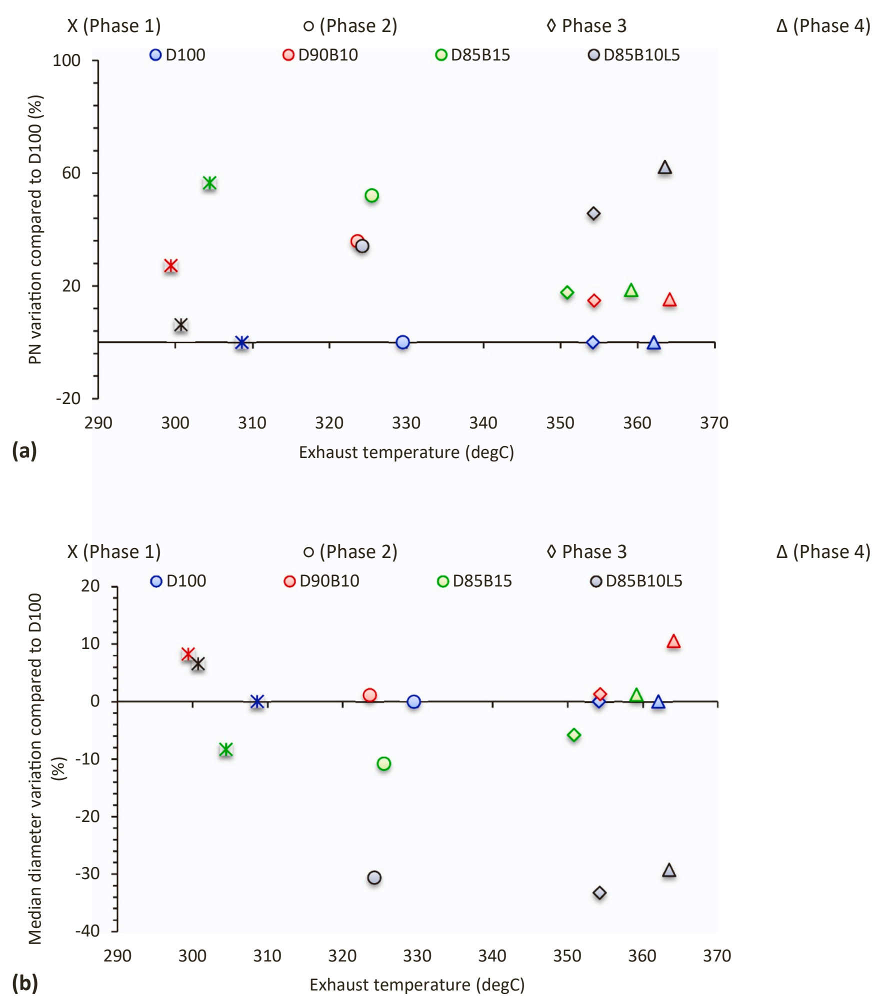

Fig. 8. (a) Particulate number concentration and (b) count median diameter changes compared to D100 at different exhaust temperatures within 4 phases of engine warm-up with D100, D90B10, D85B15 and D85B10L5.

compared to diesel [90]. Fig. 4(a) shows that the difference between cold-start and hot-operation was lower for the fuel blends than for D100. Moreover, increasing the share of biofuel in the blend decreased the PN variation, as illustrated in Fig. 4(a), in which, when compared to D90B10, D85B15 had lower variations in different phases. However, it could be a misleading conclusion, and data should be studied from another perspective. As shown in Fig. 8(a), when compared to D100, using D90B10 and D85B15 increased the PN within all phases, particularly during cold-start. During Phase 1, as compared to pure diesel, utilising biofuel blends increased PN (27–57%), while within the hot operation (Phase 4), the increase was 4–19%. This observation is of importance as after-treatment systems are less effective during cold-start, which is a regular part of daily driving. The higher viscosity of biofuels (which has an adverse impact on fuel evaporation and atomisation [98] and the increased number of small particles could be some reasons for the increased PN during cold-start. Additionally, the higher oxygen content in biofuels could lead to higher PN. This is because biofuels have higher oxygen in the centre of the diffusion flame where HC concentration is higher, resulting in an increase in smaller size particles [51]. Fig. 8(b) illustrates the negative impact of biofuel usage. It demonstrates that during the initial two phases, the emitted particles' median diameter by D85B15 is smaller than D100. This indicates that using 15% biofuels in the blend emits finer particles during cold-start when the after-treatment systems are not yet effective. This is concerning because smaller particle size has been linked to increased toxicity [30].

Fig. 9 depicts the cumulative particles share in all phases, indicating an increase in smaller particles when using fuel blends instead of D100 during cold-start. The percentage of sub-50 nm particles was higher for the fuel blends, with D85B15 having the highest share of 29% in Phase 1. This is similar to sub-23 nm particles, with D85B15 showing an increase from 1% to 9% in Phase 1. This increase in nucleation mode particles could be attributed to the higher concentration of VOCs found in biofuels in comparison with diesel [20,90].

The results show that in Phases 3 and 4, D85B10L5 has the highest PN compared to other fuels. Fig. 5(a) illustrates that the nucleation mode particles' share when using the fuel blend with 5% lubrication oil (D85B10L5) has a significant increase as the engine warms up, which is again concerning from a health and toxicity point of view. This increase can be explained by the particle size, where smaller particles tend to contribute more to PN, and larger particles contribute more to PM. As shown, the particles' median diameter with this fuel in Phase 4 is around 50 nm, while the median diameter is above 80 nm with the other tested fuels. This notably reduced the median diameter in comparison with other tested fuels, which is the reason for the increased PN. According to Kittelson et al. [41], the lubricating oil's sulphur content increases nanoparticles. Particles in nucleation mode—mainly formed within the exhaust gas dilution&cooling process—are composed of soluble&volatile organic fractions which are formed from the evaporated lubricating oil and fuel that escape from the oxidation process. Therefore, nucleation mode particles can be potentially increased by higher evaporated lubricating oil. Within cold-start, the low temperatures of fuel and cylinder wall can adversely impact fuel vaporisation and lubricating oil, which leads to fewer particles in the nucleation mode. However, with the elevated engine temperature, the charge air temperature in the cylinder rises, and therefore, it can lead to better vaporisation of fuel and oil, which can increase the particles in the nucleation mode consequently. Since lubricating oil presence during combustion can affect the particles in nucleation mode, the fuel blend with 5% lubricating oil has more particles in the nucleation mode when compared to D100 within the engine warming up period.

It should be noted that the effect of using biofuel on CMD was only a few nanometers (Fig. 3) and not significant compared to the error bars shown in the figure. The most significant changes were observed for lubricating oil addition to the fuel, as seen in Fig. 4(b). However, this lube oil effect originated from the formation of nucleation mode, shown in Fig. 5(a).

3.3. Practical implications

The cost and negative health effects associated with fossil fuels have led to an increased focus on the use of biofuels, with measures put in place to promote their usage. However, vehicle emissions continue to be a concern, and governments are implementing tighter emission regulations to limit the amount of pollution from vehicles. This study reveals that during the cold-start period, which frequently occurs in daily

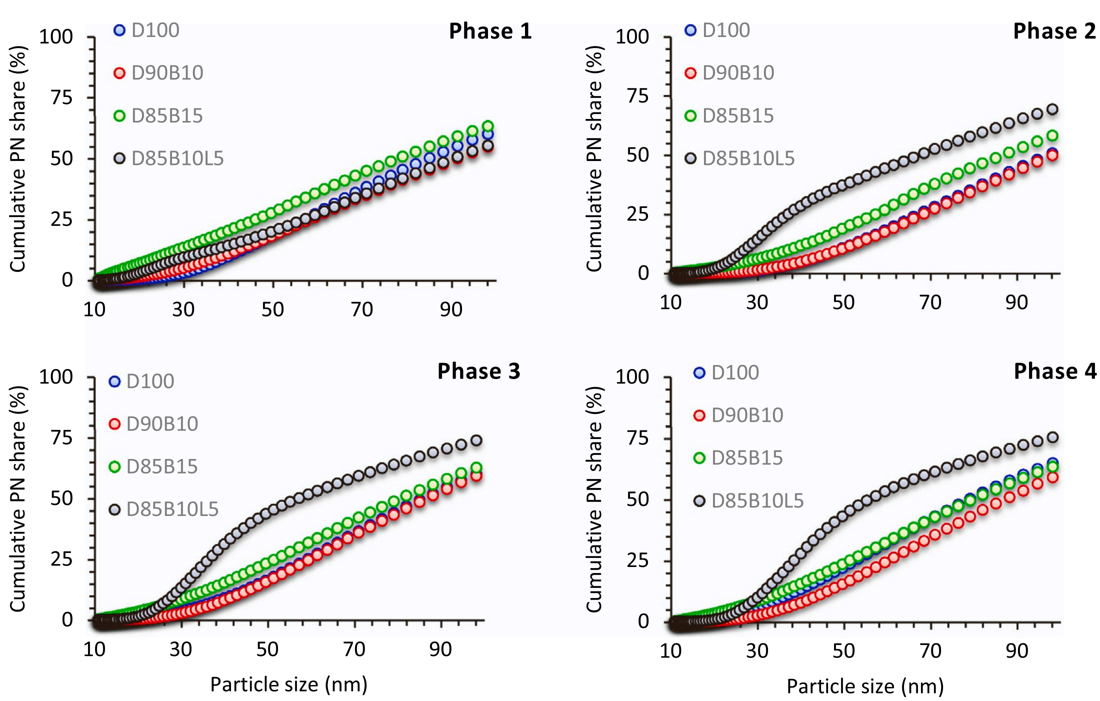

Fig. 9. Cumulative share of particulate number within 4 phases of engine warm-up with D100, D90B10, D85B15 and D85B10L5.

driving, in which vehicle emissions are not effectively treated by after-treatment systems [99], the use of biofuels leads to an increase in smaller particles that are more toxic. While current regulations (e.g. Euro 6.2) disregard particles with sizes less than 23 nm, this research showed that a significant proportion of particles during cold-start are sub-23 nm. The current rising share of utilising biofuel in the market can elevate the number of such small particles, which is a concern from a health point of view. Also, it can be seen that as the engine warms up, the dilution and mix of lubrication oil with the fuel in the engine can lead to a significant increase in the number of particles, including small particles in nucleation mode. This is also a concern that should motivate car manufacturers to improve their engine design to avoid this mixing. However, amending the current regulations to take into account the small particles will indirectly force car manufacturers to find a solution so that they can pass the vehicle certification tests when it comes to PN emissions.

The study suggests that considering sub-23 nm particles in regulation would increase the number of particles during vehicle emissions certification tests, and many cars may not be able to comply with the current threshold for PN emissions. This study highlights that with current regulations, failing or passing the vehicle homologation tests cannot address the fact that the already certified vehicles in towns emit a significant amount of small particles that can adversely affect people's health. The study concludes that future regulations should include smaller particles, or the current regulations should be amended to include them. Also, during the type approval vehicle certification tests, as well as the emission limits for the whole drive cycle, regulations should put a limit on cold-start emissions. It is understood that cold-start operation is a part of the driving cycles when it comes to homologation tests; however, some vehicles only operate within cold-start. For example, driving a short distance between home and work. Another example of the importance and significance of cold-start emissions can be when the parents drop their kids at school every morning when their cars are still cold. Such emissions from cold-start can impact children's health. This study used a 6-cylinder turbocharged diesel engine. Given that a significant portion of vehicles on roads use diesel engines, and some are 6-cylinder turbocharged, the results of this study can be valid. It should also be clarified that the intention of this study was not to mimic real-world conditions directly but rather to isolate and analyse specific emission characteristics under controlled parameters. The choice of laboratory conditions helped to precisely control variables and obtain meaningful insights into particle emissions under controlled settings. While the differences between laboratory conditions and real-world scenarios are acknowledged, the controlled nature of this study provides a foundational understanding of the emissions characteristics.

4. Conclusions

Using a 6-cylinder, turbocharged Cummins diesel engine, the study aimed to investigate the impact of biofuel and lubricating oil (as sources of nanoparticles) on the concentration, PM and PN median diameter and size distribution, and their cumulative share at different size ranges during four different phases of cold-start and warm-up operation. 10% and 15% biofuel and 5% lubricating oil were added to the fuel. This study categorised the engine warm-up period into cold-start, hot-start and two intermediate phases, which cannot be considered as official cold-start or hot-start by the regulations. Results revealed that:

- PN for all the fuels increased, and particle size decreased during the engine warm-up period. PN during hot-start was up to 132% higher compared to cold-start.
- During Phase 1 (cold-start), the PN median diameter for tested fuels was 79–94 nm. In Phase 2, the particles tend to have higher PN and bigger particles than in Phase 1 due to the change in injection strategy. The nucleation mode particle share in Phase 4 was higher in comparison with Phase 3 due to the impact of sub-optimal engine oil temperature in Phase 3.
- Compared to the cold-start phase, the rate of PN concentration increase and PN size decrease are more significant for the fuel blend with 5% lubricating oil. The median diameter of particles with this fuel in Phase 4 was around 50 nm, while for the other fuels, it was above 80 nm. The sulphur content of lubricating oil is the likely cause of an increase in nanoparticles.
- PN had an increasing trend in all phases when biofuel was used. As the engine warmed up, the PN variation compared to diesel decreased when the share of biofuel in the blend was increased. Biofuel blends emitted smaller particles during cold-start when the after-treatment systems were not effective.
- Sub-23 nm particles accounted for up to 0.1% of the PM cumulative share, while their cumulative PN share was 9%. Sub-100 nm particles accounted for 50–75% of PN, but only up to 13% of PM. It was shown that the median diameter of PM ranged from 178 to 213 nm, while the median diameter of PN ranged between 57 and 100 nm.

Environmental implications

This study focuses on unregulated hazardous fine particles emitted from vehicles, particularly highlighting the impact of increasing the share of biofuel (as mandated by current regulations), which leads to a reduction in particle size, resulting in increased particle toxicity. However, existing emissions regulations and standards disregarded small particles (diameter $<$ 23 nm) that are more toxic. The particle size reduction, therefore increased toxicity, escalates significantly during vehicle cold start operation, which is an inevitable frequent daily driving norm where after-treatment systems prove ineffective. Thus, urgent attention is required to include smaller particles in regulations to safeguard public health..

CRediT authorship contribution statement

Ali Zare: Conceptualization, Methodology, Validation, Formal analysis, Writing – original draft, Visualization, Project administration Supervision **Meisam Babaie:** Writing – review & editing, Visualization, **Alireza Shirneshan:** Conceptualization, Methodology, Writing – review & editing **Puneet Verma:** Formal analysis, Writing – review & editing **Liping Yang:** Formal analysis, Writing – review & editing, Visualization **M.M Rahman:** Methodology, Validation, Writing – review & editing **Zoran D. Ristovski:** Conceptualization, Methodology, Resources, Writing – review & editing, Funding acquisition **Richard J. Brown:** Conceptualization, Methodology, Resources, Writing – review & editing, Funding acquisition **Timothy A. Bodisco:** Software, Formal analysis, Writing – review & editing, Visualization, **Svetlana Stevanovic:** Conceptualization, Methodology, Validation, Writing – review & editing, Project administration, Supervision.

Declaration of Competing Interest

The authors declare that they have no known competing financial interests or personal relationships that could have appeared to influence the work reported in this paper.

Data availability

The data that has been used is confidential.

Acknowledgement

The authors would like to express gratitude for the assistance provided by Prof. Jochen Mueller, Mr. Andrew Elder, Mr. Doug Stuart, and Mr. Noel Hartnett, as well as the Australian Research Council (project number LP110200158).

Appendix

Based on EU Directive 2012/46/EU regulation, the cold-start duration begins from the engine start after 12-hour soak until the coolant temperature reaches 70 degC, otherwise until the first 5 min. In this study, Phase 1, which is 4 min, is within the cold-start period. It can be seen in Fig. A1 that in Phase 1, the coolant temperature and oil are increasing but still less than 70 degC. Also, the start of injection of the engine which is commanded by ECU is constant. It can be seen that when the engine temperature reaches 65 degC, the start of injection changes. This is due to the injection strategy of the tested engine, which can be slightly different for engines manufactured by different OEMs. This injection strategy change can lead to some transient behaviours. Therefore, Phase 2 in this study is dedicated to this transient engine operation in which the start of injection changes as well as the engine coolant and s phase, the engine is already warmed up. Given that this study utilised an SMPS with 2-minute sampling time, the two samples at the beginning are dedicated to Phase 1 (cold-start), the third one is dedicated to Phase 2, and the fourth and fifth were measured during Phase 3. Phase 4 consists of the last samples.

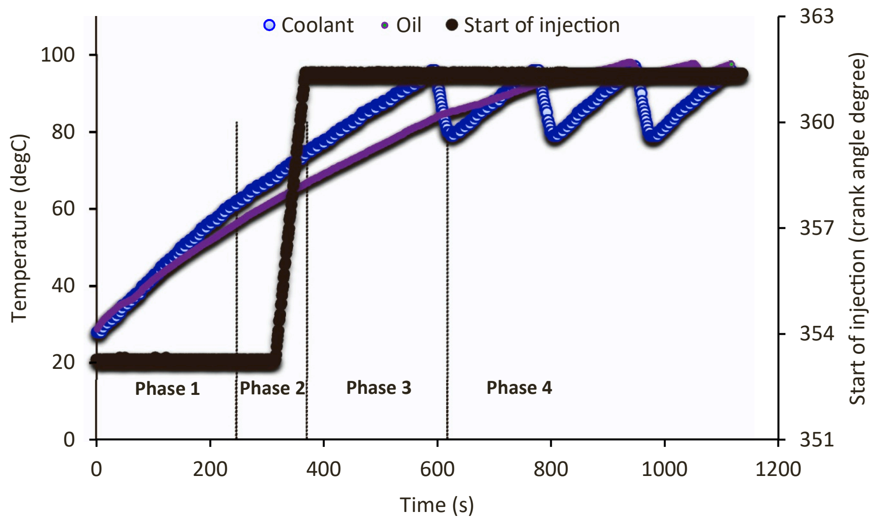

Appendix Fig. A1. Start of injection, and engine coolant & oil temperatures within cold-start and warm-up with D100.

References

[1] Joshi, A., 2020. Review of vehicle engine efficiency and emissions. SAE Int J Engines. https://doi.org/10.4271/2020-01-0352.

[2] Zare, A., Brown, R.J., Bodisco, T., 2021. *Ethanol Fumigation and Engine Performance in a Diesel Engine*, in *Alcohol as an Alternative Fuel for Internal Combustion Engines*. Springer,, pp. 191–212.

[3] Yang, L., Zare, A., Bodisco, T.A., Nabi, N., Liu, Z., Brown, R.J., 2021. Analysis of cycle-to-cycle variations in a common-rail compression ignition engine fuelled with diesel and biodiesel fuels. Fuel 290, 120010.

[4] Salek, F., Babaie, M., Shakeri, A., Hosseini, S.V., Bodisco, T., Zare, A., 2021. Numerical study of engine performance and emissions for port injection of ammonia into a gasoline\ethanol dual-fuel spark ignition engine. Appl Sci 11 (4), 1441.

[5] Yang, L.-P., Bodisco, T.A., Zare, A., Marwan, N., Chu-Van, T., Brown, R.J., 2019. Analysis of the nonlinear dynamics of inter-cycle combustion variations in an ethanol fumigation-diesel dual-fuel engine. Nonlinear Dyn 95, 2555–2574.

[6] Jafari, M., Verma, P., Bodisco, T.A., Zare, A., Surawski, N.C., Borghesani, P., et al., 2019. Multivariate analysis of performance and emission parameters in a diesel engine using biodiesel and oxygenated additive. Energy Convers Manag 201, 112183.

[7] Verma, T.N., Shrivastava, P., Rajak, U., Dwivedi, G., Jain, S., Zare, A., et al., 2021. A comprehensive review of the influence of physicochemical properties of biodiesel on combustion characteristics, engine performance and emissions. J Traffic Transp Eng 8 (4), 510–533.

[8] Arora, P., Verma, P., Lodi, F., Jafari, M., Zare, A., Stevanovic, S., et al., 2023. Particulate emissions and soot characterisation of diesel engine exhaust for steady-state operating condition using dioctyl phthalate blends with diesel. Fuel 340, 127527.

[9] Zare, A., Bodisco, T.A., Nabi, M.N., Hossain, F.M., Ristovski, Z.D., Brown, R.J., 2017. Engine performance during transient and steady-state operation with oxygenated fuels. Energy fuels 31 (7), 7510–7522.

[10] Datta, A., Mandal, B.K., 2016. A comprehensive review of biodiesel as an alternative fuel for compression ignition engine. Renew Sustain Energy Rev 57, 799–821. https://doi.org/10.1016/j.rser.2015.12.170.

[11] Redel-Macías, M.D., Pinzi, S., Babaie, M., Zare, A., Cubero-Atienza, A., Dorado, M. P., 2021. Bibliometric studies on emissions from diesel engines running on alcohol/diesel fuel blends. A case study about noise emissions. Processes 9 (4), 623.

[12] Zare, A., Nabi, M.N., Bodisco, T.A., Hossain, F.M., Rahman, M.M., Ristovski, Z.D., et al., 2016. The effect of triacetin as a fuel additive to waste cooking biodiesel on engine performance and exhaust emissions. Fuel 182, 640–649. https://doi.org/10.1016/j.fuel.2016.06.039.

[13] Nabi, M.N., Zare, A., Hossain, F.M., Rahman, M.M., Bodisco, T.A., Ristovski, Z.D., et al., 2016. Influence of fuel-borne oxygen on European Stationary Cycle: diesel engine performance and emissions with a special emphasis on particulate and NO emissions. Energy Convers Manag 127, 187–198. https://doi.org/10.1016/j.enconman.2016.09.010.

[14] Lodi, F., Zare, A., Arora, P., Stevanovic, S., Ristovski, Z., Brown, R.J., et al., 2023. Engine performance characteristics using microalgae derived dioctyl phthalate biofuel during cold, preheated and hot engine operation. Fuel 344, 128162.

[15] Nabi, M.N., Zare, A., Hossain, F.M., Ristovski, Z.D., Brown, R.J., 2017. Reductions in diesel emissions including PM and PN emissions with diesel-biodiesel blends. J Clean Prod 166, 860–868. https://doi.org/10.1016/j.jclepro.2017.08.096.

[16] Nabi, M.N., Zare, A., Hossain, F.M., Bodisco, T.A., Ristovski, Z.D., Brown, R.J., 2017. A parametric study on engine performance and emissions with neat diesel and diesel-butanol blends in the 13-Mode European Stationary Cycle. Energy Convers Manag 148, 251–259. https://doi.org/10.1016/j.enconman.2017.06.001.

[17] Nabi, N., A. Zare, M. Hossain, M.M. Rahman, D. Stuart, Z. Ristovski, R. Brown. Formulation of new oxygenated fuels and their influence on engine performance and exhaust emissions. The Combustion Institute Australia and New Zealand Section.

[18] Verma, P., Stevanovic, S., Zare, A., Dwivedi, G., Chu Van, T., Davidson, M., et al., 2019. An overview of the influence of biodiesel, alcohols, and various oxygenated additives on the particulate matter emissions from diesel engines. Energies 12 (10), 1987.

[19] World Health Organization, Review of evidence on health aspects of air pollution–REVIHAAP Project. 2013.

[20] Hedayat, F., Stevanovic, S., Milic, A., Miljevic, B., Nabi, M.N., Zare, A., et al., 2016. Influence of oxygen content of the certain types of biodiesels on particulate oxidative potential. Sci Total Environ 545, 381–388.

[21] Vaughan, A., Stevanovic, S., Morrison, L., Pourkhesalian, A.M., Rahman, M., Zare, A., et al., 2015. Removal of organic content from diesel exhaust particles alters cellular responses of primary human bronchial epithelial cells cultured at an air-liquid interface. J Environ Anal Toxicol 5 (5) (p. Article-number).

[22] Stevanovic, S., Vaughan, A., Hedayat, F., Salimi, F., Rahman, M.M., Zare, A., et al., 2017. Oxidative potential of gas phase combustion emissions-An underestimated

and potentially harmful component of air pollution from combustion processes. Atmos Environ 158, 227–235.
[23] Vaughan, A., Stevanovic, S., Banks, A.P., Zare, A., Rahman, M.M., Bowman, R.V., et al., 2019. The cytotoxic, inflammatory and oxidative potential of coconut oil-substituted diesel emissions on bronchial epithelial cells at an air-liquid interface. Environ Sci Pollut Res 26 (27), 27783–27791.
[24] Vaughan, A., Stevanovic, S., Rahman, M., Zare, A., Miljevic, B., Ristovski, Z., et al., 2016. N-acetyl cysteine (NAC) intervention attenuates the effects of diesel and biodiesel emission exposure on human bronchial epithelial cells, 16HBE, at air-liquid interface. Eur Respir J.
[25] Vaughan, A., Stevanovic, S., Zare, A., Rahman, M., Miljevic, B., Ristovski, Z., et al., 2016. Coconut oil substitution in diesel fuel alters human bronchial epithelial cell responses to diesel emission exposure at the air–liquid interfacein vitro: to 022. Respirology 21.
[26] Wong, P.K., Ghadikolaei, M.A., Chen, S.H., Fadairo, A.A., Ng, K.W., Lee, S.M.Y., et al., 2022. Physical, chemical, and cell toxicity properties of mature/aged particulate matter (PM) trapped in a diesel particulate filter (DPF) along with the results from freshly produced PM of a diesel engine. J Hazard Mater 434, 128855. https://doi.org/10.1016/j.jhazmat.2022.128855.
[27] Hüftlein, F., Seidenath, D., Mittereder, A., Hillenbrand, T., Brüggemann, D., Otti, O., et al., 2023. Effects of diesel exhaust particles on the health and survival of the buff-tailed bumblebee Bombus terrestris after acute and chronic oral exposure. J Hazard Mater 458, 131905. https://doi.org/10.1016/j.jhazmat.2023.131905.
[28] Delphi Technologies, *Worldwide emissions standards-Passenger cars and light duty vehicles.* Delphi, 2019. 〈https://www.delphi.com/innovations〉.
[29] Chen, L., Stone, R., Richardson, D., 2012. A study of mixture preparation and PM emissions using a direct injection engine fuelled with stoichiometric gasoline/ethanol blends. Fuel 96, 120–130.
[30] Chen, L., Ding, S., Liu, H., Lu, Y., Li, Y., Roskilly, A.P., 2017. Comparative study of combustion and emissions of kerosene (RP-3), kerosene-pentanol blends and diesel in a compression ignition engine. Appl Energy 203, 91–100.
[31] Chen, L., Raza, M., Xiao, J., 2017. Combustion analysis of an aviation compression ignition engine burning pentanol–kerosene blends under different injection timings. Energy Fuels 31 (9), 9429–9437.
[32] Zare, A., Bodisco, T.A., Nabi, M.N., Hossain, F.M., Rahman, M.M., Ristovski, Z.D., et al., 2017. The influence of oxygenated fuels on transient and steady-state engine emissions. Energy 121, 841–853. https://doi.org/10.1016/j.energy.2017.01.058.
[33] Jafari, M., Verma, P., Bodisco, T.A., Zare, A., Surawski, N.C., Borghesani, P., et al., 2019. Multivariate analysis of performance and emission parameters in a diesel engine using biodiesel and oxygenated additive. Energy Convers Manag 201, 112183. https://doi.org/10.1016/j.enconman.2019.112183.
[34] Chen, L., Hu, X., Wang, J., Yu, Y., 2019. Impacts of alternative fuels on morphological and nanostructural characteristics of soot emissions from an aviation piston engine. Environ Sci Technol 53 (8), 4667–4674.
[35] Krahl, J., Bünger, J., Schröder, O., Munack, A., Knothe, G., 2002. Exhaust emissions and health effects of particulate matter from agricultural tractors operating on rapeseed oil methyl ester. J Am Oil Chem' Soc 79 (7), 717–724.
[36] ACEA. ACEA proposals for Euro 7 and Euro VII emission standards. 2022 [cited 2023 14/08/2023]; Available from: 〈https://www.acea.auto/publication/acea-proposals-for-euro-7-and-euro-vii-emission-standards/〉.
[37] Thessalonikis, A.P., 2019. Measuring automotive exhaust particles down to 10 nanometres. SOCIETAL CHALLENGES - Smart, Green Integr Transp. https://doi.org/10.3030/724085.
[38] Guido, C., Di Maio, D., Napolitano, P., Beatrice, C., 2022. Sub-23 particle control strategies towards Euro VII HD SI natural gas engines. Transp Eng 10, 100132.
[39] McClellan, R.O., Hesterberg, T.W., Wall, J.C., 2012. Evaluation of carcinogenic hazard of diesel engine exhaust needs to consider revolutionary changes in diesel technology. Regul Toxicol Pharmacol 63 (2), 225–258.
[40] Leach, F., Lewis, A., Akehurst, S., Turner, J., Richardson, D., 2019. Sub-23 nm particulate emissions from a highly boosted GDI engine. SAE Tech Pap 0148–7191.
[41] Kittelson, D., Watts, W., Johnson, J., Thorne, C., Higham, C., Payne, M., et al., 2008. Effect of fuel and lube oil sulfur on the performance of a diesel exhaust gas continuously regenerating trap. Environ Sci Technol 42 (24), 9276–9282.
[42] Tornehed, P., Olofsson, U., 2011. Lubricant ash particles in diesel engine exhaust. Literature review and modelling study. Proc Inst Mech Eng, Part D: J Automob Eng 225 (8), 1055–1066.
[43] Pirjola, L., Karjalainen, P., Heikkila, J., Saari, S., Tzamkiozis, T., Ntziachristos, L., et al., 2015. Effects of fresh lubricant oils on particle emissions emitted by a modern gasoline direct injection passenger car. Environ Sci Technol 49 (6), 3644–3652.
[44] Kittelson, D.B., M. Arnold W.F., Watts, Review of diesel particulate matter sampling methods. (1999): University of Minnesota, Department of Mechanical Engineering, Center for …
[45] Bodek, K.M., V.V. Wong, The Effects of Sulfated Ash, Phosphorus and Sulfur on Diesel Aftertreatment Systems-A Review. SAE Technical Paper, 2007. 0148–7191.
[46] Reiter, M.S., Kockelman, K.M., 2016. The problem of cold starts: a closer look at mobile source emissions levels. Transp Res Part D: Transp Environ 43, 123–132.
[47] André, M., 1991. In actual use car testing: 70,000 kilometers and 10,000 trips by 55 French cars under real conditions. SAE Trans 65–72.
[48] Lodi, F., Zare, A., Arora, P., Stevanovic, S., Jafari, M., Ristovski, Z., et al., 2020. Combustion analysis of a diesel engine during warm up at different coolant and lubricating oil temperatures. Energies 13 (15), 3931.
[49] Alalo, A.M.A., Babaie, M., Shirneshan, A., Bodisco, T.A., Ristovski, Z.D., Brown, R.J., et al., 2022. Exergy and energy analysis during cold-start and warm-up engine operation. Fuel 330, 125580.
[50] Zare, A., Bodisco, T.A., Nabi, M.N., Hossain, F.M., Ristovski, Z.D., Brown, R.J., 2018. A comparative investigation into cold-start and hot-start operation of diesel engine performance with oxygenated fuels during transient and steady-state operation. Fuel 228, 390–404. https://doi.org/10.1016/j.fuel.2018.05.004.
[51] Giakoumis, E.G., Rakopoulos, C.D., Dimaratos, A.M., Rakopoulos, D.C., 2012. Exhaust emissions of diesel engines operating under transient conditions with biodiesel fuel blends. Prog Energy Combust Sci 38 (5), 691–715. https://doi.org/10.1016/j.pecs.2012.05.002.
[52] Verma, P., Jafari, M., Zare, A., Pickering, E., Guo, Y., Osuagwu, C.G., et al., 2021. Soot particle morphology and nanostructure with oxygenated fuels: a comparative study into cold-start and hot-start operation. Environ Pollut 275, 116592.
[53] Zare, A., Nabi, M.N., Bodisco, T.A., Hossain, F.M., Rahman, M.M., Chu Van, T., et al., 2017. Diesel engine emissions with oxygenated fuels: a comparative study into cold-start and hot-start operation. J Clean Prod 162, 997–1008. https://doi.org/10.1016/j.jclepro.2017.06.052.
[54] Lodi, F., Zare, A., Arora, P., Stevanovic, S., Jafari, M., Ristovski, Z., et al., 2020. Engine performance and emissions analysis in a cold, intermediate and hot start diesel engine. Appl Sci 10 (11), 3839.
[55] Nam, E., 2008. Analysis of particulate matter emissions from light-duty gasoline vehicles in Kansas City. US Environmental Protection Agency,.
[56] Song, W.W., Fang, W.X., Liu, H., Li, W.L., Zhang, Z., Li, C.H., et al., 2023. Enhanced diesel emissions at low ambient temperature: hazardous materials in fine particles. J Hazard Mater 449, 131011. https://doi.org/10.1016/j.jhazmat.2023.131011.
[57] Lee, D.-W., J. Johnson, J. Lv, K. Novak, J. Zietsman, Comparisons between vehicular emissions from real-world in-use testing and EPA moves estimation. Texas Transportation Institute, 2012.
[58] Van, T.C., Zare, A., Jafari, M., Bodisco, T.A., Surawski, N., Verma, P., et al., 2019. Effect of cold start on engine performance and emissions from diesel engines using IMO-Compliant distillate fuels. Environ Pollut 255, 113260.
[59] Mitchell, B.J., Zare, A., Bodisco, T.A., Nabi, M.N., Hossain, F.M., Ristovski, Z.D., et al., 2017. Engine blow-by with oxygenated fuels: a comparative study into cold and hot start operation. Energy 140, 612–624.
[60] Cao, Y., 2007. Operation and cold start mechanisms of internal combustion engines with alternative fuels. SAE Technol Pap 0148–7191.
[61] Roberts, A., Brooks, R., Shipway, P., 2014. Internal combustion engine cold-start efficiency: a review of the problem, causes and potential solutions. Energy Convers Manag 82, 327–350.
[62] Zare, A., Bodisco, T.A., Verma, P., Jafari, M., Babaie, M., Yang, L., et al., 2020. Emissions and performance with diesel and waste lubricating oil: a fundamental study into cold start operation with a special focus on particle number size distribution. Energy Convers Manag 209, 112604.
[63] Guido, C., Napolitano, P., Alfuso, S., Corsetti, C., Beatrice, C., 2021. How engine design improvement impacts on particle emissions from an HD SI natural gas engine. Energy 231, 120748.
[64] Lapuerta, M., Ramos, Á., Barba, J., Fernández-Rodríguez, D., 2018. Cold-and warm-temperature emissions assessment of n-butanol blends in a Euro 6 vehicle. Appl Energy 218, 173–183.
[65] Ko, J., Jin, D., Jang, W., Myung, C.-L., Kwon, S., Park, S., 2017. Comparative investigation of NOx emission characteristics from a Euro 6-compliant diesel passenger car over the NEDC and WLTC at various ambient temperatures. Appl Energy 187, 652–662.
[66] Ramos, Á., García-Contreras, R., Armas, O., 2016. Performance, combustion timing and emissions from a light duty vehicle at different altitudes fueled with animal fat biodiesel, GTL and diesel fuels. Appl Energy 182, 507–517.
[67] Bodisco, T., Brown, R.J., 2013. Inter-cycle variability of in-cylinder pressure parameters in an ethanol fumigated common rail diesel engine. Energy 52, 55–65.
[68] Bodisco, T., Tröndle, P., Brown, R.J., 2015. Inter-cycle variability of ignition delay in an ethanol fumigated common rail diesel engine. Energy 84, 186–195.
[69] TSI, Aerosol Instrument Manager® Software for Scanning Mobility Particle Sizer™ (SMPS™) Spectrometer. 2010, TSI. p. 71.
[70] Kittelson, D.B., 1998. Engines and nanoparticles: a review. J Aerosol Sci 29 (5–6), 575–588.
[71] Giechaskiel, B., Lähde, T., Gandi, S., Keller, S., Kreutziger, P., Mamakos, A., 2020. Assessment of 10-nm particle number (PN) portable emissions measurement systems (PEMS) for future regulations. Int J Environ Res Public Health 17 (11), 3878.
[72] Kittelson, D.B., Watts, W.F., Johnson, J.P., Thorne, C., Higham, C., Payne, M., et al., 2008. Effect of fuel and lube oil sulfur on the performance of a diesel exhaust gas continuously regenerating trap. Environ Sci Technol 42 (24), 9276–9282.
[73] Zare, A., Bodisco, T.A., Verma, P., Jafari, M., Babaie, M., Yang, L., et al., 2020. Emissions and performance with diesel and waste lubricating oil: a fundamental study into cold start operation with a special focus on particle number size distribution. Energy Convers Manag 209, 112604.
[74] Zare, A., Bodisco, T.A., Verma, P., Jafari, M., Babaie, M., Yang, L., et al., 2022. Particulate number emissions during cold-start with diesel and biofuels: a special focus on particle size distribution. Sustain Energy Technol Assess 51, 101953.
[75] Andersson, J., Preston, H., Warrens, C., Brett, P., 2004. Fuel and lubricant effects on nucleation mode particle emissions from a Euro III light duty diesel vehicle. SAE Trans 1387–1402.
[76] Miller, A., Ahlstrand, G., Kittelson, D., Zachariah, M., 2007. The fate of metal (Fe) during diesel combustion: morphology, chemistry, and formation pathways of nanoparticles. Combust Flame 149 (1), 129–143. https://doi.org/10.1016/j.combustflame.2006.12.005.
[77] Frusteri, F., Spadaro, L., Beatrice, C., Guido, C., 2007. Oxygenated additives production for diesel engine emission improvement. Chem Eng J 134 (1–3), 239–245.

[78] Lodi, F., Zare, A., Arora, P., Stevanovic, S., Verma, P., Jafari, M., et al., 2021. Characteristics of particle number and particle mass emissions of a diesel engine during cold-, warm-, and hot-start operation. SAE Technol Pap 0148–7191.
[79] Shahariar, G.M.H., Bodisco, T.A., Zare, A., Sajjad, M., Jahirul, M.I., Van, T.C., et al., 2022. Impact of driving style and traffic condition on emissions and fuel consumption during real-world transient operation. Fuel 319, 123874.
[80] Bodisco, T., Zare, A., 2019. Practicalities and driving dynamics of a real driving emissions (RDE) Euro 6 regulation homologation test. Energies 12 (12), 2306.
[81] Delphi. Worldwide emissions standards. 2018 [cited 2019 15/04/2019]; Available from: 〈https://www.delphi.com/innovations#emissionstandards〉.
[82] Zare, A., Bodisco, T.A., Jafari, M., Verma, P., Yang, L., Babaie, M., et al., 2021. Cold-start NOx emissions: diesel and waste lubricating oil as a fuel additive. Fuel 286, 119430. https://doi.org/10.1016/j.fuel.2020.119430.
[83] Chien, S.-M., Huang, Y.-J., Chuang, S.-C., Yang, H.-H., 2016. Effects of biodiesel blending on particulate and polycyclic aromatic hydrocarbon emissions in nano/ultrafine/fine/coarse ranges from diesel engine. Aerosol Air Qual Res 9 (1), 18–31.
[84] Yusuf, A.A., Inambao, F.L., 2019. Effect of cold start emissions from gasoline-fueled engines of light-duty vehicles at low and high ambient temperatures: recent trends. Case Stud Therm Eng 14, 100417. https://doi.org/10.1016/j.csite.2019.100417.
[85] Lodi, F., Zare, A., Arora, P., Stevanovic, S., Ristovski, Z., Brown, R.J., et al., 2023. Combustion characteristics of microalgae-based dioctyl phthalate biofuel during ambient, preheated and hot engine operation. Fuel 331, 125890.
[86] Lodi, F., Zare, A., Arora, P., Stevanovic, S., Ristovski, Z.D., Brown, R.J., et al., 2022. Gaseous and particulate emissions analysis using microalgae based dioctyl phthalate biofuel during cold, warm and hot engine operation. Fuel 312, 122965.
[87] Arora, P., F. Lodi, P. Verma, M. Jafari, A. Zare, S. Stevanovic, et al., Structural characterisation of soot particles for cold-start and hot-start operation of a diesel engine. 2020.
[88] Kasper, M., 2005. Sampling and measurement of nanoparticle emissions for type approval and field control. SAE Technol Pap 0148–7191.
[89] Tsai, J.-H., Chang, S.-Y., Chiang, H.-L., 2012. Volatile organic compounds from the exhaust of light-duty diesel vehicles. Atmos Environ 61, 499–506.
[90] Pourkhesalian, A.M., Stevanovic, S., Salimi, F., Rahman, M.M., Wang, H., Pham, P. X., et al., 2014. Influence of fuel molecular structure on the volatility and oxidative potential of biodiesel particulate matter. Environ Sci Technol 48 (21), 12577–12585.
[91] Hosseinzadeh-Bandbafha, H., Li, C., Chen, X., Peng, W., Aghbashlo, M., Lam, S.S., et al., 2022. Managing the hazardous waste cooking oil by conversion into bioenergy through the application of waste-derived green catalysts: a review. J Hazard Mater 424, 127636. https://doi.org/10.1016/j.jhazmat.2021.127636.
[92] Yilmaz, N., Davis, S.M., 2022. Formation of polycyclic aromatic hydrocarbons and regulated emissions from biodiesel and n-butanol blends containing water. J Hazard Mater 437, 129360. https://doi.org/10.1016/j.jhazmat.2022.129360.
[93] Cheng, M.-T., Chen, H.-J., Young, L.-H., Yang, H.-H., Tsai, Y.I., Wang, L.-C., et al., 2015. Carbonaceous composition changes of heavy-duty diesel engine particles in relation to biodiesels, aftertreatments and engine loads. J Hazard Mater 297, 234–240. https://doi.org/10.1016/j.jhazmat.2015.04.076.
[94] Zhang, Z.-H., Balasubramanian, R., 2014. Physicochemical and toxicological characteristics of particulate matter emitted from a non-road diesel engine: comparative evaluation of biodiesel-diesel and butanol-diesel blends. J Hazard Mater 264, 395–402. https://doi.org/10.1016/j.jhazmat.2013.11.033.
[95] Khan, M.M., Kadian, A.K., Sharma, R.P., Hasnain, S.M.M., Mohamed, A., Ragab, A. E., et al., 2023. Emission reduction and performance enhancement of CI Engine propelled by neem biodiesel-neem oil-decanol-diesel blends at high injection pressure. Sustainability 15 (11), 9084.
[96] Salek, F., Babaie, M., Redel-Macias, M.D., Ghodsi, A., Hosseini, S.V., Nourian, A., et al., 2020. The effects of port water injection on spark ignition engine performance and emissions fueled by pure gasoline, E5 and E10. Processes 8 (10), 1214.
[97] Odibi, C., Babaie, M., Zare, A., Nabi, M.N., Bodisco, T.A., Brown, R.J., 2019. Exergy analysis of a diesel engine with waste cooking biodiesel and triacetin. Energy Convers Manag 198, 111912.
[98] Armas, O., Hernández, J.J., Cárdenas, M.D., 2006. Reduction of diesel smoke opacity from vegetable oil methyl esters during transient operation. Fuel 85 (17–18), 2427–2438.
[99] Zare, A., Stevanovic, S., Jafari, M., Verma, P., Babaie, M., Yang, L., et al., 2021. Analysis of cold-start NO2 and NOx emissions, and the NO2/NOx ratio in a diesel engine powered with different diesel-biodiesel blends. Environ Pollut 290, 118052.